ARTICLE

Aqueous Solution Behavior of Anionic Fluorene-*co*-thiophene-Based Conjugated Polyelectrolytes

Hugh D. Burrows,*,† María J. Tapia,*,‡ Sofia M. Fonseca,† Artur J. M. Valente,† Victor M. M. Lobo,† Licínia L. G. Justino,† Song Qiu,§ Swapna Pradhan,§ Ullrich Scherf,§ Nitin Chattopadhyay,⊥ Matti Knaapila,¶ and Vasil M. Garamus#

Departamento de Química and Centro de Neurociências e Biologia Celular, Universidade de Coimbra, 3004-535 Coimbra, Portugal, Departamento de Química, Universidad de Burgos, Plaza Misael Bañuelos s/n, Burgos 09001, Spain, Makromolekulare Chemie, Bergische Universität Wuppertal, DE-42097 Wuppertal, Germany, Department of Chemistry, Jadavpur University, Kolkata 700 032, India, Department of Physics, Institute for Energy Technology, NO-2027 Kjeller, Norway, MAX-Lab, Lund University, SE-22100, Lund, Sweden, and GKSS Research Centre, DE-21502 Geesthacht, Germany

ABSTRACT Two anionic fluorene−thiophene alternating copolymers, poly[9,9-bis(4-sulfonylbutoxyphenyl)fluorene-2,7-diyl-2,5-thienylene] (PBS-PFT) and poly[9,9-bis(4-sulfonylbutoxyphenyl)fluorene-2,7-diyl-2,2′-bithiophene-5,5′-diyl] (PBS-PF2T), have been synthesized and their solution behaviors in water studied by UV−vis absorption spectroscopy, fluorescence, and electrical conductivity and compared with that of the previously studied conjugated polyelectrolyte (CPE) poly[9,9-bis(4-sulfonylbutoxyphenyl)fluorene-2,7-diyl-1,4-phenylene] (PBS-PFP). These conjugated polymers do not form solutions at the molecular level in water but instead form clusters. Information on the structure of these clusters for PBS-PF2T comes from small-angle X-ray and neutron scattering. The relative ease of dispersing the copolymers in water increases with an increase in the number of thiophene rings in these alternating copolymers. Semiempirical calculations on the structure suggest that this results from bending of the chains and increased conformational flexibility, decreasing interchain interactions. These CPEs can be dissolved in water at the molecular level using the nonionic surfactants *n*-dodecylpentaoxyethylene glycol ether ($C_{12}E_5$) or Triton X-100 to obtain systems with increased photoluminescence quantum yield and increased electrical conductivity that can be solution-processed for potential applications as components of sensory or optoelectronic devices.

KEYWORDS: conjugated polyelectrolytes • solution processing • fluorene−thiophene copolymers • polyelectrolyte aggregation

INTRODUCTION

Conjugated organic polymers are currently finding real or potential applications in areas as diverse as organic and biological sensors (1), field effect transistors, photovoltaic cells, organic semiconductor lasers, and various light-emitting devices (2, 3). Much of this has been stimulated by the first report by Friend and co-workers in 1990 of conjugated polymer electroluminescence from a poly(*p*-phenylenevinylene) (PPV) layer sandwiched between indium−tin oxide and metal electrodes (4). Since then, a large number of other polymer-based light-emitting diodes (PLEDs) and electrochemical cells have been developed using various PPV derivatives, poly(fluorene)s, poly(*p*-phenyleneethynylene)s, poly(thiophene)s, and poly(carbazole)s (5). PLED-based displays are already in the market in mobile phones, watches, personal music systems, televisions, etc.

The rigid poly(fluorene) backbone has proved particularly useful in this area because of its blue emission, high fluorescence quantum yield, thermal and chemical stability, and reasonable solubility in various solvents (6). Its properties can be modulated both on the backbone by copolymerization (6c) and on side chains by the attachment of different functional groups at the 9 position of the fluorene five-membered ring (7). Poly(thiophene)s are another important family of electroactive and photoactive polymers. Unsubstituted poly(thiophene)s are insoluble and infusible materials, but the polymers can be made soluble and their optical properties tuned by substitution in the 3 and 4 positions, which allows emission over the whole visible spectrum from red to blue with solution photoluminescence efficiencies of up to 40% (5, 8). With poly(thiophene)s, the luminescence yield is frequently limited by efficient intersystem crossing induced by the heavy atom effect of sulfur (9) and is further drastically reduced in the solid state because of interchain interactions (5, 10). However, the high yields of formation of triplet states may be advantageous (11, 12) and may

* E-mail: burrows@ci.uc.pt (H.D.B.), mjtapia@ubu.es (M.J.T.). Phone: +351+239+854482 (H.D.B.), +34 947258061 (M.J.T.). Fax: +351 +239+827703 (H.D.B.), +34 94728831 (M.J.T.).
Received for review December 23, 2008 and accepted February 23, 2009
† Universidade de Coimbra.
‡ Universidad de Burgos.
§ Bergische Universität Wuppertal.
⊥ Jadavpur University.
¶ Institute for Energy Technology and Lund University.
# GKSS Research Centre.
DOI: 10.1021/am800267n

Published on Web 03/20/2009

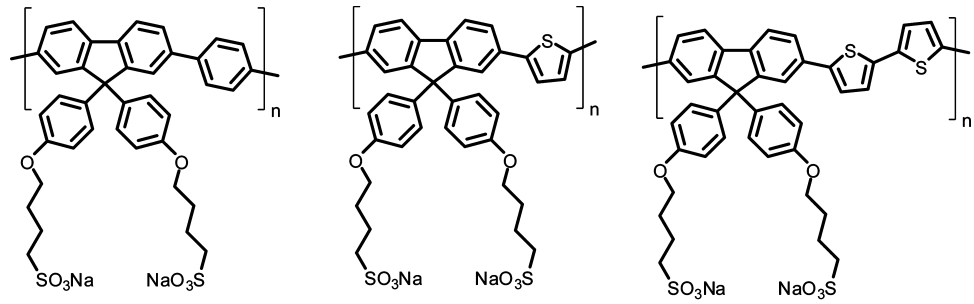

FIGURE 1. Structures of alternating CPEs studied.

possibly be exploited through electrophosphorescent devices (13). In addition, thiophene-based (co)polymers are important materials for charge transport and are finding applications in areas such as field-effect transistors (14) and photovoltaic systems (15).

The complementary structural, optical, spectroscopic, and electronic properties of these two moieties have stimulated interest in the exploitation of fluorene–thiophene copolymers, for obtaining materials with excellent emission properties and good charge injection/transport (5, 6c, 6f, 6g, 16). Some of the earliest studies on alternating fluorene-based copolymers came from the Dow Chemical group (6e, 14), while Lévesque, Leclerc, and co-workers (17) and other groups (18)have shown that it is possible to efficiently tune the emission colors from blue to green and yellow in these systems by introducing various (oligo)thiophene units. Other authors have reported a systematic study of the structure–property relationship of fluorene–thiophene-based conjugated polymers (5, 19, 28). For device applications, poly(dialkylfluorene-*alt*-bithiophene) copolymers (as F8T2 with *n*-octyl substituents) are of particular interest as active components in both photovoltaic systems (20) and field-effect transistors (3b, 21).

In addition to modifications to their conjugated backbone, conjugated polymers and copolymers can be modified by the introduction of ionic side chains, which, in principle, will make them soluble in water and/or alcohols and so improve their processability using techniques such as ink-jet and screen printing (22). Such conjugated polyelectrolytes (CPEs) are finding applications in sensing or electroluminescent devices and as charge-injection and/or transport layers (23). In addition, it is possible to form novel heterostructures with such CPEs through layer-by-layer self-assembly with other polymers or surfactants (24). We have previously reported the photophysics, spectroscopy, and electrical conductivity of the anionic poly[9,9-bis(4-sulfonylbutoxyphenyl)fluorene-2,7-diyl-1,4-phenylene] (PBS-PFP; Figure 1) and have shown that although it does not dissolve in pure water because of cluster formation, it can be solubilized using organic cosolvents (25) or surfactants (26), leading to enhancement in its fluorescence quantum yield. With the nonionic *n*-dodecylpentaoxyethylene glycol ether ($C_{12}E_5$) (26a, 26b, 27), the cationic lecithin mimic (1-*O*-(L-arginyl)-2,3-*O*-dilauroyl-*sn*-glycerol dichlorhydrate (1212R), (26c) or the gemini surfactants α,ω-$\{(C_mH_{2m+1}N^+(CH_3)_2)\}_2(CH_2)_s)Br_2$ (e.g., 12-6-12) (26d), the CPE is incorporated as a single isolated chain into mixed polymer–surfactant aggregates. This results in an increase in the emission quantum yield, a blue shift in the fluorescence spectrum, and a better resolved vibronic structure.

We extend these studies to two alternating fluorene–thiophene-based anionic CPEs, poly[9,9-bis(4-sulfonylbutoxyphenyl)fluorene-2,7-diyl-2,5-thienylene] (PBS-PFT) and poly[9,9-bis(4-sulfonylbutoxyphenyl)fluorene-2,7-diyl-2,2′-bithiophene-5,5′-diyl] (PBS-PF2T), whose structures are given in Figure 1. We report their syntheses, characterization, and detailed structural, spectroscopic, photophysical, and electrical conductance studies in water, and compare their behavior with that of PBS-PFP. These copolymers also tend to form clusters in water, and with PBS-PF2T we provide hints on the structures of these based on small-angle X-ray (SAXS) and neutron (SANS) scattering measurements. Furthermore, we report the effect of nonionic alkyloxyethylene surfactants on their solution behavior in water. We also highlight potential applications of these materials in optical sensing, light-emitting devices, and bulk-heterojunction solar cells.

EXPERIMENTAL SECTION

Materials. The nonionic surfactants *n*-dodecylpentaoxyethylene glycol ether ($C_{12}E_5$) and Triton X-100 and the fullerene C_{60} were acquired from Aldrich and used as received. The synthesis of poly[9,9-bis(4-sulfonylbutoxyphenyl)fluorene-2,7-diyl-1,4-phenylene] (PBS-PFP; Figure 1) has been previously described (26b). Other reagents were of the purest grades available and used as received. Solutions of PBS-PFP, poly[9,9-bis(4-sulfonylbutoxyphenyl)fluorene-2,7-diyl-2,5-thienylene] (PBS-PFT), and poly[9,9-bis(4-sulfonylbutoxyphenyl)fluorene-2,7-diyl-2,2′-bithiophene-5,5′-diyl] (PBS-PF2T) were prepared in Milli-Q Millipore water with concentrations of 6×10^{-3}, 0.012, and 0.016 g L^{-1}, respectively, by stirring overnight. All samples were kept in the absence of light. For neutron scattering, the polymer PBS-PF2T was dissolved in D_2O (D, 99.9%) supplied by Cambridge Isotope Laboratories, Inc.

Synthesis of 2,7-Dibromo-9,9-bis(4-sulfonylbutoxyphenyl)fluorene (Dibromo Monomer). The dibromo monomer 2,7-dibromo-9,9-bis(4-sulfonylbutoxyphenyl)fluorene was synthesized in three steps. The first step involved oxidation of 2,7-dibromofluorene with sodium dichromate/acetic acid to 2,7-dibromofluoren-9-one. In the second step, 2,7-dibromofluoren-9-one was reacted with phenol/methanesulfonic acid to give 2,7-dibromo-9,9-bis(4-hydroxyphenyl)fluorene, while the last step involved etherification of 2,7-dibromo-9,9-bis(4-hydroxyphenyl)fluorene with 1,4-butane sultone to 2,7-dibromo-9,9-bis(4-

Scheme 1. Synthesis of (top) PBS-PFT and (bottom) PBS-PF2T

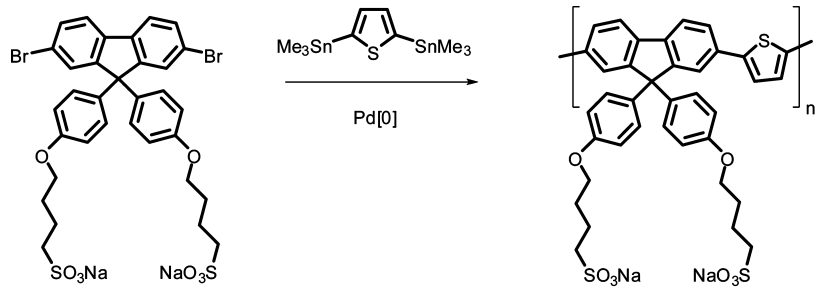

PBS-PFT

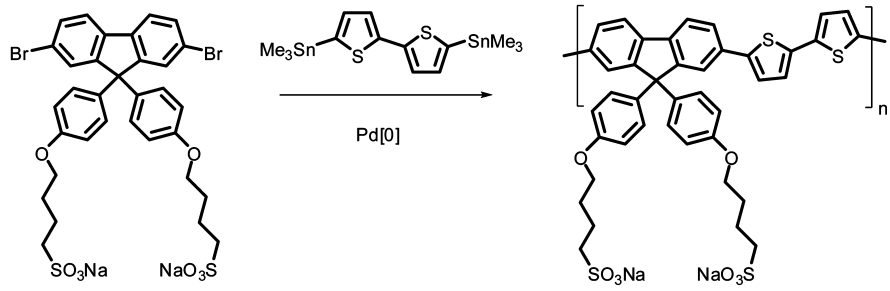

PBS-PF2T

sulfonylbutoxyphenyl)fluorene in dioxane/NaOH. The monomer was obtained in 71% yield (over three steps).

Synthesis of PBS-PFT and PBS-PF2T. PBS-PFT was prepared as shown in Scheme 1.

A solution of 2,5-bis(trimethylstannyl)thiophene (28) (0.4097 g, 1 mmol), 2,7-dibromo-9,9-bis(4-sulfonylbutoxyphenyl)fluorene (0.8245 g, 1 mmol), and $Pd(PPh_3)_4$ (40 mg) was refluxed in 25 mL of dry toluene for 4 days under argon. After cooling to room temperature, 50 mL of toluene were added. The resulting polymer formed a dispersion in water. The aqueous layer was isolated and the water removed to give a yellow solid. The residue was redissolved in water and purified by dialysis against a dialysis membrane with a cutoff at $M_n = 3500$ to yield 350 mg (42 %) of PBS-PFT. The polymer was characterized by ^{1}H NMR spectroscopy (400 MHz, DMSO): $\delta(^1H)$ [ppm] 6.0−7.6 (ar-H), 3.1−3.7 (α,δ-CH_2), 0.9−2.0 (β,γ-CH_2). Gel permeation chromatography (GPC) analysis in *N*,*N*-dimethylformamide (DMF) gave a M_n of ca. 1800 g mol^{-1} (universal calibration, UV−vis detection at 364 nm). However, because of interactions of the polyelectrolyte with the column material, the M_n value is likely to be considerably underestimated.

PBS-PF2T was synthesized as shown in Scheme 1. A solution of 5,5′-bis(trimethylstannyl)-2,2′-bithiophene (28) (0.492 g, 1 mmol), 2,7-dibromo-9,9-bis(4-sulfonylbutoxyphenyl)fluorene (0.8245 g, 1 mmol), and $Pd(PPh_3)_4$ (40 mg) was refluxed in 25 mL of dry toluene for 4 days under argon. Workup and purification were similar to those of the above-mentioned PBS-PFT. PBS-PF2T was obtained as a reddish solid (500 mg, 64%). The polymer was characterized by ^{1}H NMR spectroscopy (400 MHz, DMSO): $\delta(^1H)$ [ppm] 6.55−7.9 (ar-H), 3.1−4.45 (α,δ-CH_2), 0.9−2.0 (β,γ-CH_2). GPC analysis in DMF gave a M_n of ca. 3300 g mol^{-1} (universal calibration, UV−vis detection at 364 nm). However, because of interactions of the polyelectrolyte with the column material, the M_n value is almost certainly underestimated.

Apparatus and Methods. ***Spectroscopic Measurements.*** Absorption and luminescence spectra were recorded on Shimadzu UV-2100 absorption and Jobin-Ivon SPEX Fluorolog 3-22 fluorescence spectrometers, respectively. Fluorescence spectra were corrected for the wavelength response of the system. Fluorescence quantum yields were measured using quinine sulfate in 1 M sulfuric acid as the standard (29) for PBS-PFP and α-pentathiophene (α5) in benzene (30) and dioxane (31) for PBS-PFT and PBS-PF2T, respectively.

Fluorescence decays were measured using a home-built time-correlated single photon counting apparatus with a nitrogen-filled IBH 5000 coaxial flashlamp as the excitation source, a Jobin-Ivon monochromator, a Philips XP2020Q photomultiplier, and Canberra Instruments time-to-amplitude converter and multichannel analyzer. Alternate measurements (1000 counts per cycle), controlled by *Decay* software (Biodinâmica, Portugal), of the pulse profile at 337 or 356 nm and the sample emission were performed until $(1-2) \times 10^4$ counts at the maximum were reached (32). The fluorescence decays were analyzed using the modulating functions method of Striker with automatic correction for the photomultiplier "wavelength shift" (33).

SAXS and SANS Studies. SAXS measurements were performed at I711 beamline at MAX-lab in Lund, Sweden (34). The X-ray energy was 11.3 keV, the sample-to-detector distance 1325 mm, and the q range 0.009−0.15 Å^{-1}. The beam size was 0.25 mm × 0.25 mm. The samples were measured in Hilgenberg glass mark tubes, which had inner diameters of about 1.5 mm and wall thicknesses of 10 μm. These were placed in a thermostatic holder (Julabo). The absolute intensity scale was calibrated using water.

SANS measurements were performed using the SANS-1 instrument at the GKSS Research Centre in Geesthacht, Germany (35). The overall q range was from 0.006 to 0.3 Å^{-1}. The samples were filled in Hellma quartz cells of 2 mm path length and placed in a thermostatic holder (Julabo). The raw scattering patterns were corrected for sample transmission, room background, and sample cell scattering. The isotropic two-dimensional scattering patterns were azimuthally averaged, converted

to an absolute scale, and corrected for detector efficiency by dividing by the incoherent scattering spectra of 1-mm-thick pure water. The scattering from D_2O used for the sample preparation was subtracted as a background; the small incoherent scattering due to the nondeuterated polymer was taken into account by the fitting procedure.

The scattering functions of solutions were interpreted using scaling concepts. The simple interpretation was enhanced by numerical modeling by indirect Fourier transforms (IFTs) according to Glatter (36) as well as by simulated annealing according to Svergun (37).

Electrical Conductivity. Solution electrical resistances were measured with a Wayne-Kerr model 4265 Automatic LCR meter at 1 kHz. A Shedlovsky-type conductance cell was used (38). The cell constant (approximately 0.3328 cm^{-1}) was determined to ±0.02% from measurements with KCl (reagent grade, recrystallized and dried using the procedure and data from Barthel et al.) (39). Measurements were made at 25.00 ± 0.01 °C in a Grant thermostat bath, as described in detail elsewhere (26b).

Semiempirical Calculations. Semiempirical quantum mechanical calculations were performed for the PBS-PFP, PBS-PFT, and PBS-PF2T tetramers using the *MOPAC2007* (40) system of programs (in the gas phase). The structures were optimized using the PM6 (41) Hamiltonian and the EF routine. In the structures, the alkylic chains at the 9 positions were replaced by methyl groups for the sake of reducing the time of computation. It has been demonstrated that the presence of the alkyl groups at the 9 position does not significantly affect the equilibrium geometries or the electronic structure of fluorene derivatives (42, 43).

RESULTS AND DISCUSSION

Synthesis and Characterization. The copolymers PBS-PFT and PBS-PF2T were prepared by Stille-type aryl−aryl cross couplings and purified by dialysis against membranes with a cutoff at 3500. The molecular weights in both cases could not be unambiguously determined. There were serious difficulties in obtaining accurate average molecular weights using GPC in DMF because of interactions of the polyelectrolytes with the column material. The obtained values for PBS-PFT and PBS-PF2T, respectively ($\overline{M}_n$'s of ca. 1800 and 3300 g mol^{-1}; polydispersity index of ca. 2.0), have to be considered as the lower limits.

Both PBS-PFT and PBS-PF2T could be dispersed in water, with "solubilities" considerably greater than that found for PBS-PFP. These follow the order PBS-PF2T > PBS-PFT > PBS-PFP. As will be discussed later, incorporation of the thiophene moiety probably increases the solubility in water both because this unit is more polar than the 1,4-phenylene group in PBS-PFP (44) and because the fluorene−thiophene chains have greater conformational flexibility than fluorene−phenylene chains (45). For PBS-PF2T, the solubility is sufficient to obtain information on the nature of the polymer−water system using SAXS and SANS. However, we should note that with PBS-PFT, as with PBS-PFP (26a, 26b), we probably do not have a true solution at the molecular level because there is a tendency to precipitate upon standing. In addition, although PBS-PF2T does not precipitate, as we will see later, there are strong indications from SAXS that this exists in water as extended polymer clusters.

Absorption and Fluorescence Spectroscopy. The normalized absorption and emission spectra of aqueous dispersions of the three polymers PBS-PFT, PBS-PF2T, and PBS-PFP are shown in Figure 2.

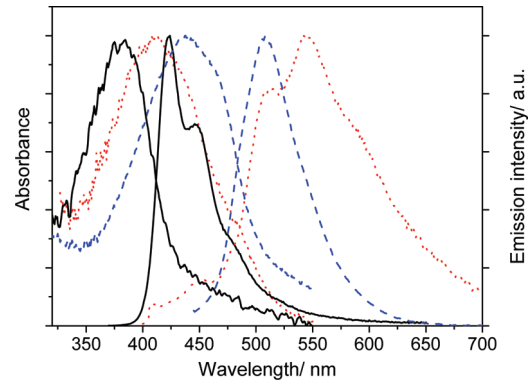

FIGURE 2. Normalized absorption and emission spectra of PBS-PFP (solid line, 6×10^{-3} g L^{-1}), PBS-PFT (dashed line, 2×10^{-2} g L^{-1}), and PBS-PF2T (dotted line, 1.6×10^{-2} g L^{-1}).

As was observed for the corresponding nonionic fluorene-based alternating copolymers (12, 18a, 18b, 28), replacement of 1,4-phenylene by 2,5-thiophene units leads to a red shift in both absorption and emission maxima. With the fluorescence spectra, this shift is, as expected, larger for PBS-PF2T than for PBS-PFT. The unexpected blue shift of the absorption maxima when going from PBS-PFT to PBS-PF2T (Figure 2) is a result of the increased "solubility" of PBS-PF2T in water. In contrast to the "solid-state-like" absorption spectrum of PBS-PFT with its long-wavelength scattering tail, PBS-PF2T exhibits a more "solution-like" spectrum with a weak aggregate shoulder in the high-energy region and the absence of the long-wavelength scattering tail, as observed for PBS-PFP and PBS-PFT. Such pronounced solvatochromic responses are typical for thiophene-based homo- and copolymers (8d). This difference in the absorption spectra is also reflected in the much better structured fluorescence spectrum of PBS-PF2T. With the UV−vis absorption spectra, the Beer−Lambert law is followed in a wide concentration range. In the case of PBS-PFP, this is true up to the stock polymer concentration of 6×10^{-3} g L^{-1}. With the thiophene copolymers, a linear increase of the absorbance as a function of the polymer concentration is observed up to ca. 2×10^{-2} g L^{-1}, reflecting their greater "solubilities". Data for PBS-PFT are shown in Figure 3. Absorption and fluorescence maxima, emission quantum yields, and lifetimes of these three polymers are summarized in Table 1.

The absorption spectra of both PBS-PFT and PBS-PF2T show broad maxima in the 400−450 nm region, with no indications of absorption due to separate thiophene units, in agreement with complete conjugation between the fluorene and thiophene units. The fluorescence spectra are similar to those of the corresponding nonionic copolymers (18a, 18b, 28) and show a red shift in the emission maxima and a decrease in the fluorescence quantum yield upon incorporation of the thiophene rings. The decrease in the emission efficiency is particularly dramatic in aqueous dispersions of PBS-PF2T and may hint at relatively strong interchain interactions, coupled with increased intersystem crossing due to enhanced spin−orbit coupling induced by the sulfur atoms (11, 12).

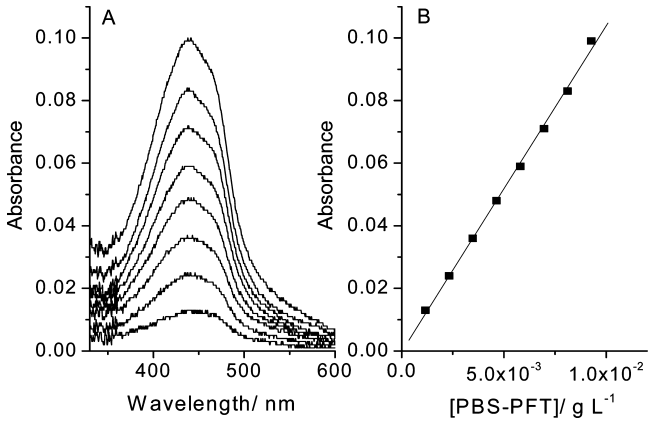

FIGURE 3. (A) Absorption spectra at several polymer concentrations (1.16, 2.32, 3.48, 4.64, 5.80, 6.96, 8.12, and 9.28 mg L^{-1}) and (B) Beer–Lambert plot for PBS-PFT in water.

Table 1. Average Polymer Molecular Weight, $\overline{M}_n$, Absorption and Emission Maxima and Shoulders, Emission Quantum Yield, ϕ, and Fluorescence Lifetimes, τ, in Water

polymer	$\overline{M}_n$/g mol^{-1} [a]	absorption/ nm	emission maxima/ nm	emission shoulders/ nm	ϕ	τ/ns
PBS-PFP	~6500	381	423	446, 479	0.23	0.36
PBS-PFT	~1800	280, 319, 440	507		0.03	≤1.2
PBS-PF2T	~3300	280, 319, 412	542	588	0.006	0.92

[a] Determined by GPC.

Conductimetric Results. As with previous studies on aqueous dispersions of fluorene-based CPEs (26a, 26b, 46), electrical conductivity can provide valuable information on the aggregation behavior in these systems. We have studied the effect of the concentration on the electrical conductivity of PBS-PFT and PBS-PF2T in water. The molar conductivity (Λ) was calculated using

$$\Lambda = (\kappa - \kappa_0)/(c \times 1000) \quad (1)$$

κ and κ_0 are electrolytic conductivities of the solution and solvent, respectively, and c is the polymer concentration. As can be seen from Figure 4, for a similar polyelectrolyte concentration range, the molar conductivities depend on the square root of the concentration, in agreement with the Kohlrausch equation (38)

$$\Lambda = \Lambda^0 - Ac^{1/2} \quad (2)$$

The molar limiting conductivities Λ^0 are reported in Table 2 and are of magnitudes similar to those found for PBS-PFP (26a, 26b) and for other polyelectrolytes in aqueous solution (46c, 47). The fact that the behavior of aqueous solutions of PBS-PFT and PBS-PF2T, with respect to both the Beer–Lambert and Kohlrausch laws, is similar to that expected with small species suggests that the polymer aggregates may be considered as separate chemical entities.

Because of solubility problems, it was not possible to study PBS-PFP and the fluorene–thiophene CPEs over the same concentration range. However, although their behaviors are qualitatively similar, there are quantitative differences. The value of Λ^0 for PBS-PFT is about 1.4 times greater than that found for PBS-PF2T and about 2.2 times that of PBS-PFP (Λ^0 = 0.362 S m^2 mol^{-1}, $\overline{M}_n$ = 6500 g mol^{-1}, $M_{monomer}$ = 740.79 g mol^{-1}, and number of repeat units = 8.8 (26b)). Although data are available only for three polymers, a reasonable linear relationship is found between the value of Λ^0 and the number of monomer units [Λ^0 = 0.9 (±0.1) − 0.06 (±0.02)$n_{monomer}$]. Electrical conductivity in these CPEs will depend on the polyelectrolyte structure, charge, and counterions. With PBS-PFT, PBS-PF2T, and PBS-PFP, the side chains, and hence degrees of dissociation of sodium counterions, are the same. Therefore, although these three CPEs are aggregated in water, we believe that the limiting electrical conductivity may be used as a measure of the molecular weight of these conjugates. Further work is in progress to test this with a variety of fluorene-based CPEs.

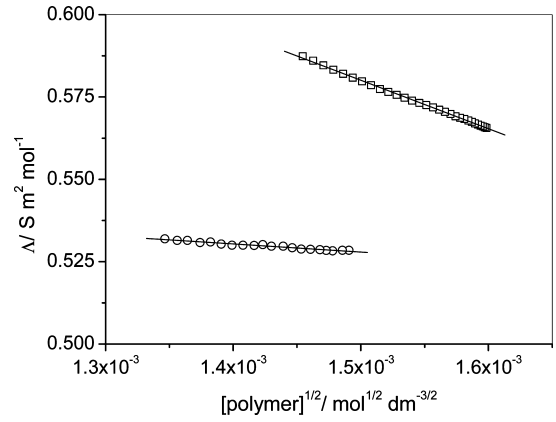

FIGURE 4. Molar electrical conductivity of PBS-PFT (□) and PBS-PF2T (○) as a function of the square root of the polymer molar concentration, in aqueous solutions, at 25 °C.

Table 2. Electrical Conductivity Data for Aqueous Dispersions of PBS-PFT and PBS-PF2T

	$\overline{M}_n$/g mol^{-1}	$M_{monomer}$/ g mol^{-1}	$n_{monomer}$	Λ^0/S m^2 mol^{-1}	slope (A)/S m^2 mol^{-1} $M^{-0.5}$
PBS-PFT	1800	746.82	2.4	0.801 (±0.002)	147 (±1)
PBS-PF2T	3300	828.94	4.0	0.565 (±0.002)	25 (±1)

A further interesting point is that the slope of Λ vs [polymer]$^{1/2}$ for PBS-PFT is 6 times greater than that for PBS-PF2T. Possibly upon an increase in the polymer concentration, interaction between PBS-PFT chains becomes more important than that for PBS-PF2T and, consequently, the molar conductivity is more affected. This may well be associated with the tendency for PBS-PFT to phase separate from water, whereas PBS-PF2T continues to stay in solution, although, as we shall show in the next section, it is in the form of clusters.

SAXS and SANS Studies on PBS-PF2T in Water. Further information on the structure of PBS-PF2T in water comes from SAXS and SANS experiments. Molar conductivity measurements point to polymer aggregation and suggest that these aggregates plausibly grow on the nanometer scale in this solvent system. If the samples

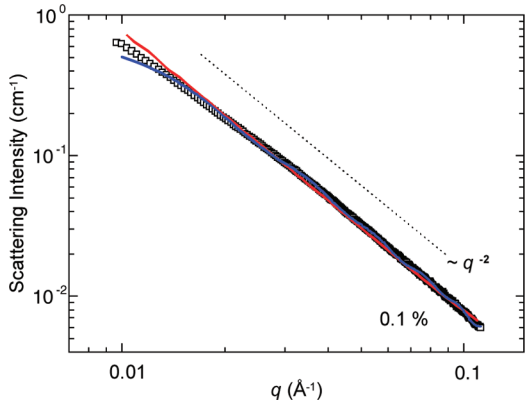

FIGURE 5. SAXS data of the PBS-PF2T polymer dissolved in 1 mg mL^{-1} water (open squares) at 25.0 ± 0.7 °C. The red solid line shows the sheetlike model fitted to the data. The blue solid line shows the scattering curve of a structure obtained by simulated annealing (vide infra). The dashed line shows a −2 decay for comparison.

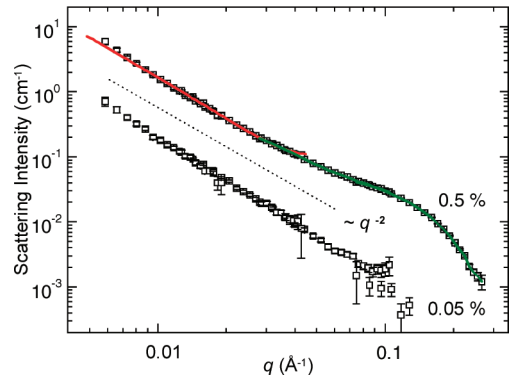

FIGURE 6. SANS data of the PBS-PF2T polymer dissolved in 5 mg mL^{-1} (open squares; upper curve) and 0.5 mg mL^{-1} (open squares; lower curve) D_2O at 25.0 ± 0.5 °C. The red and green solid lines show respectively the sheetlike and cylindrical IFT models fitted to the data below and above 0.04 Å^{-1}. The dashed line shows −2 decay for comparison.

contain scattering length density inhomogeneities greater than ∼1 nm, the scattering of X-rays and neutrons should become observable in the small-angle region, typically 2θ of less than 2°. This has motivated us to carry out small-angle scattering measurements.

Figure 5 plots the SAXS data of a PBS-PF2T polymer dissolved in water with a concentration of 1 mg mL^{-1} (∼0.1 %) and fits to the data with sheetlike and ribbon-like structural models. Strong scattering and distinctive decay of slope −2 is seen for the whole observation window, suggesting either Gaussian coils or predominantly two-dimensional aggregates. A further choice of the model can be made by considering the molecular structure of PBS-PF2T with an overall length of ∼6.4 nm. Analysis of the scattering data by a Gaussian coil model gives the value for the radius of gyration on the order of 300 nm, which is far away from the size of the molecule. This is why we may exclude the Gaussian coil model. Moreover, π conjugation results in a semirigid polymer backbone-suppressing coiling tendency. Elsewhere, sheetlike aggregates are observed for a diverse set of π-conjugated polymers (48), and we judge this scenario to be most plausible for PBS-PF2T in water. The model of sheetlike aggregates fitted to the data is in agreement with large (∼100 nm) sheets with a thickness of 2.5 nm.

Figure 6 plots SANS data of the PBS-PF2T polymer in D_2O with concentrations of 5 mg mL^{-1} (∼0.5 %) and 0.5 mg mL^{-1} (∼0.05 %). The data of a ∼0.05 % solution are consistent with the above-described SAXS data, but the data of a higher concentration sample depicts an additional feature at ∼0.1 Å^{-1}. This concentration effect is likely to be an interference maximum stemming from the interaction of charged polymers with increased concentration. Such effects are common for stiff π-CPEs in water (see, e.g., refs 27 and 49). In real space, this maximum would correspond to a ∼6 nm aggregate−aggregate distance. Even though this distance corresponds to the size of the individual polymer, it is unlikely that the feature stems from the internal structure of the aggregates because the contrast arises from hydrogen- and deuterium-rich domains and the aggregates are assumed to be uniform in this respect. Therefore, the feature (broad maximum) is tentatively interpreted to reflect the aggregate−aggregate distance, although more detailed studies should be performed to confirm this. In another scenario, the sample is polydisperse in its nature, giving evidence for both sheetlike (<0.04 Å^{-1}) and rodlike (>0.04 Å^{-1}) components (cf. the corresponding fits in Figure 6). In this case, the lateral size of the sheet would be >100 nm and the radius of the rodlike particle 1.2 nm.

Simulated ab initio annealing of PBS-PF2T aggregates was performed for illustration purposes. Figure 7 plots examples of so-determined particle shapes depicting a ribbon-like model whose calculated scattering curve fits reasonably well to the experimental data (an example is that shown in Figure 5). The aggregation behavior suggested by this model is very similar to that seen in molecular dynamics simulations of PBS-PFP in water (25). The simulated ab initio annealing model is based on the evaluation of the distance distribution function $p(r) = \Gamma(r)r^2$, where $\Gamma(r)$ is the characteristic function of the particle, without presumptions of the particle shape. Though qualitative, the model provides evidence for loose preferentially two-dimensional aggregates in contrast to dissolved 6-nm-long polymers or compact, three-dimensional aggregates. The model reproduces the thickness of aggregates as obtained from the sheetlike model but underestimates the maximum size of the aggregates, as indicated by a slight misfit at low q (cf. Figure 5). This is mirrored by the bending of ribbons, leading to an overall architecture resembling a "peel of an apple". This misfit should be understood against an opposite misfit of the sheetlike model, which points to the overestimation of the lateral size. Therefore, the obtained values of 30 and 100 nm should be taken as the lowest and highest limits of the aggregate size. However, this picture is an oversimplification because polydispersity or aggregate−aggregate interactions, reflected by the SANS data, are not taken into account.

Semiempirical Calculations on the Backbone Structure. Semiempirical quantum mechanical calculations were performed for the tetramers of these copolymers using the *MOPAC2007* (40) system of programs to obtain further insight into the differences in the solubility behavior

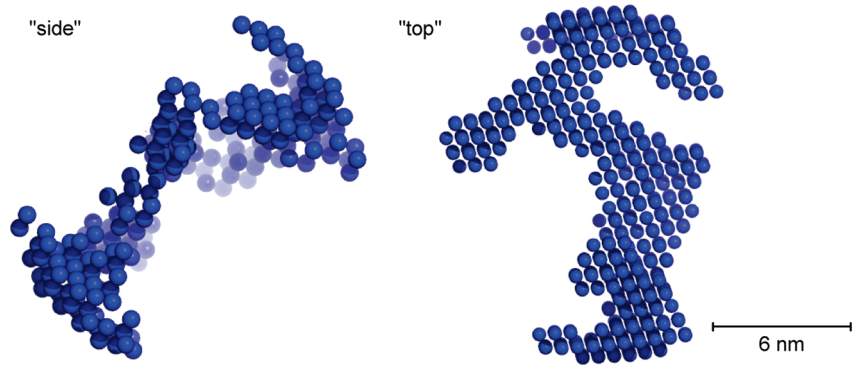

FIGURE 7. Examples of ribbon-like low-resolution structures for PBS-PF2T aggregates in water as obtained by simulated annealing. The structures are separate simulation runs and are depicted from two predominant facets: "side" and "top" views of the ribbon. The left structure corresponds to the fit shown in Figure 5. The scale bar represents the length of an individual polymer used in the experiment.

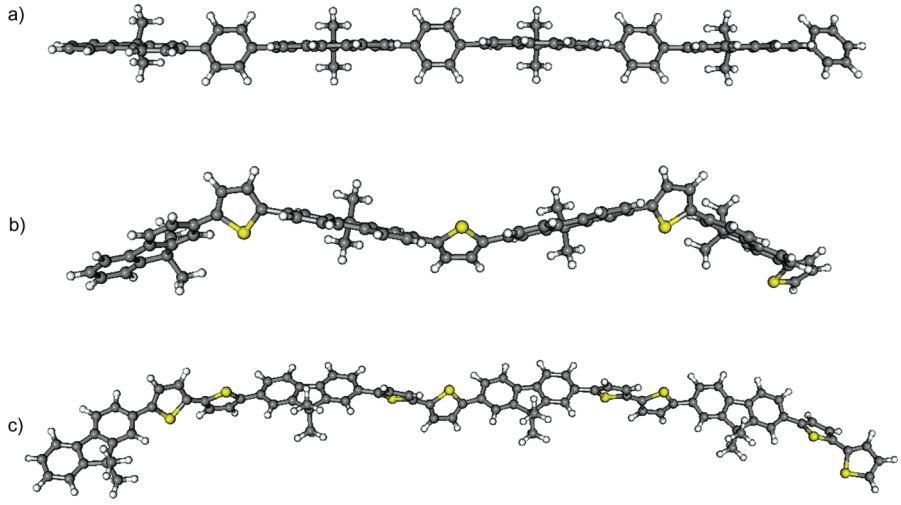

FIGURE 8. Structures of tetramers of (a) PBS-PFP, (b) PBS-PFT, and (c) PBS-PF2T obtained by semiempirical calculations.

between PBS-PFP, PBS-PFT, and PBS-PF2T. Although the alkyl chains at position 9 of the five-membered ring were replaced by methyl groups to reduce the computational time, it has been shown that this does not significantly affect the equilibrium geometries (43). The structures obtained are shown in Figure 8 and suggest that introduction of the thiophene rings in the copolymer leads to curvature in the structures and increasing conformational freedom between the alternating moieties in the copolymer. These effects are expected to reduce interchain interactions, and hence increase solubility, as observed experimentally.

Effect of $C_{12}E_5$ on the Aggregation Behavior. As indicated in the Introduction, we have shown that the aggregates formed by PBS-PFP in water are broken up by the nonionic alkyloxyethylene surfactant *n*-dodecylpentaoxyethylene glycol ether ($C_{12}E_5$) (26, 27). This leads to a blue shift in the fluorescence spectrum and dramatic increases in fluorescence quantum yields at surfactant concentrations above the critical micelle concentration (cmc). From SANS (27), SAXS (26e), and NMR studies (26b), the polymer is suggested to be present in mixed polymer−surfactant micelles as isolated PBS-PFP chains. While the mechanism of this dissolution has not yet been clarified, we favor a process where surfactants "peel-off" CPE monomers from the clusters to form micelles (26e). Alkyloxyethylene surfactants in water show phase separation (clouding) upon heating, and we have shown that interaction between these nonionic surfactants and CPEs such as PBS-PFP, PBS-PFT, or PBS-PF2T (the latter two are referred to in that paper as 1T and 2T, respectively) leads to an increase in the cloud points (44b), while the addition of sodium chloride to the surfactant/CPE/water systems decreases cloud points, indicating that interaction involves a fine balance between hydrophobic and electrostatic interactions.

To obtain more information on what is happening with the fluorene−thiophene CPEs in the presence of nonionic alkyloxyethylene surfactants, we have carried out a detailed study involving absorption, fluorescence, and electrical conductivity measurements.

Upon the addition of $C_{12}E_5$ to an aqueous dispersion of PBS-PFT [0.0116 g L^{-1} or 1.55×10^{-5} (mole repeat units) L^{-1}], a sharpening of the absorption spectrum and blue shift in the maximum was observed. This was accompanied by the appearance of some vibronic structure, which became most pronounced for concentrations around and above the cmc of the surfactant (cmc = 6.4×10^{-5} M) (50). There was also a hint of an isosbestic point for surfactant concentrations above 4.4×10^{-5} M. These changes were accompanied by a blue shift in the fluorescence, a dramatic increase in the fluorescence quantum yield, and a dramatic decrease

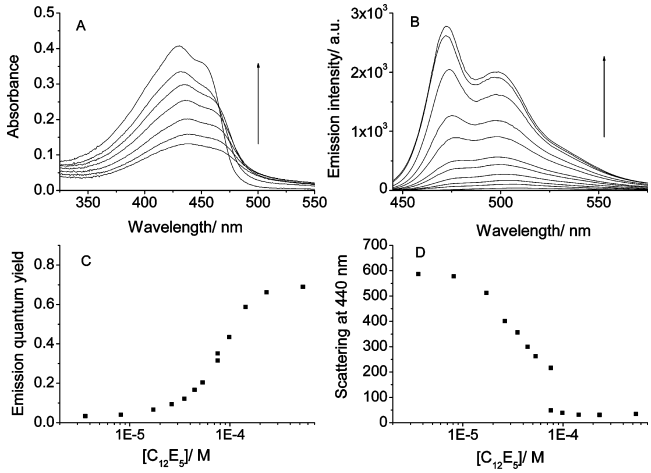

FIGURE 9. Absorption spectra ($C_{12}E_5 = 0$, 1.7×10^{-5}, 2.6×10^{-5}, 3.5×10^{-5}, 4.4×10^{-5}, 7.6×10^{-5}, and 5.3×10^{-4} M in the arrow direction; A) and fluorescence spectra ($C_{12}E_5 = 0$, 1.7×10^{-5}, 2.6×10^{-5}, 3.5×10^{-5}, 4.4×10^{-5}, 5.3×10^{-5}, 7.6×10^{-5}, 9.8×10^{-5}, 1.4×10^{-4}, 2.3×10^{-4}, and 5.3×10^{-4} M in the arrow direction; B) of PBS-PFT in water in the presence of varying concentrations of $C_{12}E_5$. The effects of the surfactant concentration (on a logarithmic scale) on the fluorescence quantum yield (C) and light scattering (D) are also shown.

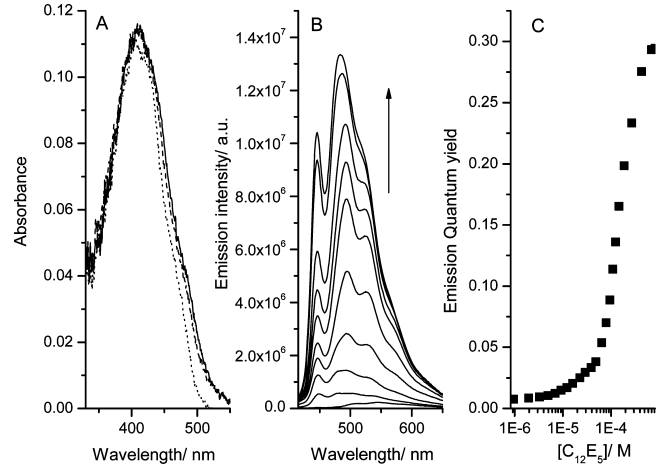

FIGURE 10. (A) Absorption spectra ($C_{12}E_5 = 0$, 4.81×10^{-5}, and 8.22×10^{-4} M as solid, dashed, and dotted lines, respectively). (B) Fluorescence spectra ($C_{12}E_5 = 0$, 1.21×10^{-5}, 4.81×10^{-5}, 7.9×10^{-5}, 1.09×10^{-4}, 1.46×10^{-4}, 1.87×10^{-4}, 2.69×10^{-4}, 4.31×10^{-4}, and 8.22×10^{-4} M, in the arrow direction). (C) Fluorescence emission quantum yield of aqueous PBS-PF2T in the presence of $C_{12}E_5$.

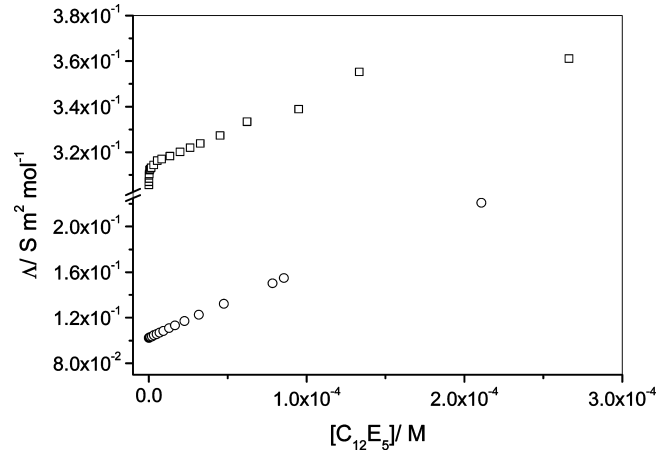

FIGURE 11. Molar conductivities of solutions of PBS-PFT (□) and PBS-PF2T (○) in the presence of $C_{12}E_5$.

in the light scattering. These results all strongly suggest that the surfactant is solubilizing PBS-PFT in a fashion similar to that seen with PBS-PFP (26a, 26b, 26e, 27), i.e., as isolated polymer chains in mixed polymer−surfactant micelles. All of these features are shown in Figure 9.

The effect of the addition of $C_{12}E_5$ to an aqueous dispersion of PBS-PF2T [0.016 g L^{-1}, 1.93×10^{-5} (mole repeat units) L^{-1}] was also studied. In this case, there was very little change in the absorption spectrum, and only modest changes in the light scattering, reflecting the greater solubility of this polymer. However, there was a blue shift in the emission accompanied by a marked increase in the quantum yield, again suggesting incorporation of the polymer in mixed surfactant−polymer aggregates. Absorption spectra and fluorescence data are shown in Figure 10.

Qualitatively, the effects of adding $C_{12}E_5$ are similar for PBS-PFT and PBS-PF2T. However, quantitatively, the effect is much more important for PBS-PFT, which is the less "soluble" polymer. Similar conclusions have been obtained from observations on the effect of these CPEs on the cloud points of aqueous alkyloxyethylene surfactant solutions (44b).

Further information was obtained from electrical conductivity measurements, as shown for both polymers in Figure 11. The presence of $C_{12}E_5$ increases the molar conductivity of both polymers, although the effect is more prominent in the case of the less soluble PBS-PFT, in agreement with what was seen in the absorption and fluorescence studies. With PBS-PFT, a marked increase in the molar conductivity of the polymer was observed for surfactant concentrations up to 4×10^{-7} M. This is similar to the behavior of PBS-PFP with Gemini surfactants (26d) and, as in that case, may be due to hydrophobic interactions between the polymer and surfactant improving the CPE solubility, and hence increasing the number of ionic species in solution. Further additions of surfactants lead to a less marked increase of the molar conductivity until the cmc is reached.

For PBS-PF2T with initial surfactant additions (below 4×10^{-7} M), the observed increase in the molar conductivity is smaller than that for PBS-PFT. This is compatible with the better solubility of PBS-PF2T (no ultrasonic bath is needed, and the decrease of the molar conductivity upon increasing polymer concentration is lower; see the previous section and slopes in Table 2). When the $C_{12}E_5$ concentration is increased, the molar conductivity also increases in a monotonous way, with no abrupt changes in the region of the cmc. This contrasts with the behavior of PBS-PFP (26a, 26b) and is probably associated with the higher solubility of PBS-PF2T as the aggregates shown in Figure 7, such that upon micellization there is no abrupt change in the ionic species released to the solution.

Comparing the changes in the molar conductivity of PBS-PFT, PBS-PF2T, and PBS-PFP, we can conclude that the interactions between PBS-PFT and $C_{12}E_5$ are intermediate

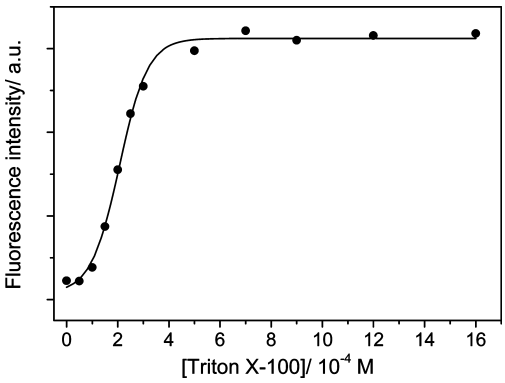

FIGURE 12. Fluorescence intensity of aqueous solutions of PBS-PF2T in the presence of Triton X-100.

between those with PBS-PFP, which is more strongly affected by the presence of the surfactant, and PBS-PF2T, such that the cmc effect is only observed for poorly soluble ionic polyfluorenes. SANS and SAXS studies will attempt to clarify the differences in the behavior between PBS-PFP and PBS-PF2T in the presence of $C_{12}E_5$.

Poly(dialkylfluorene-*alt*-bithiophene) copolymers (such as the 9,9-dioctyl compound F8T2) show potential as electron donors in both TiO_2 hybrid (20) and fullerene-based solar cells (51). To test the possible application of these solubilized CPEs in this area, we have carried out preliminary studies toward the preparation of solution-processable fullerene-based bulk-heterojunction photovoltaic devices. The fullerene C_{60} forms a stable system in aqueous solutions of the nonionic surfactant Triton X-100 (or its reduced form) (52) and, upon one-electron reduction in this medium, is transformed into a long-lived $C_{60}^{\bullet -}$ radical anion (53). In contrast, it precipitates from aqueous $C_{12}E_5$ (52). A viable photovoltaic cell using a related water-soluble poly(*p*-phenyleneethynylene)/fullerene system (54) has been demonstrated. As a prelude to seeing whether this is also possible with a water-soluble CPE/fullerene/Triton X-100 dispersion, we have studied the solubility behavior of these alternating fluorene–thiophene CPEs in water in the presence of Triton X-100. Triton X-100 is a polydisperse alkylphenoxylpoly(ethylene glycol) with an average polyoxyethylene chain length of 9.5. As with the studies using $C_{12}E_5$, upon the addition of Triton X-100 to aqueous PBS-PF2T, a blue shift was seen in the emission spectrum accompanied by a large increase in the fluorescence intensity. In this case, the marked increase in fluorescence occurs around 2×10^{-4} M (Figure 12), in agreement with the higher cmc of Triton X-100 (1.5×10^{-4} M) (55) when compared to that of $C_{12}E_5$ (6.4×10^{-5} M) (50).

The fluorescence of PBS-PF2T was studied in aqueous Triton X-100 (16 mM) in the presence of varying concentrations of C_{60}. Up to approximately 5 μM fullerene, transparent solutions were formed. Significant fluorescence quenching was seen, although detailed kinetic analysis was not attempted because it requires knowledge of the surfactant aggregation number, and the CPE and C_{60} statistical distributions between micelles under these conditions, which is beyond the scope of this work. However, observation of quenching confirms interaction between the lowest excited singlet state of the CPE and the fullerene, and although electron transfer is not the only mechanism possible, the fact that this occurs in water with the poly(*p*-phenyleneethynylene)/fullerene system (54) suggests that this is likely. We therefore feel that the PBS-PF2T/fullerene system shows a potential for photovoltaic applications, and future work will be directed toward the development of a viable system.

CONCLUSIONS

Two anionic alternating CPEs, PBS-PFT and PBS-PF2T, present interesting electronic and photonic properties, which make them potentially useful for a variety of advanced materials applications. As with the alternating anionic fluorene–phenylene CPE PBS-PFP, which we have studied in detail, these CPEs do not form true solutions in water but instead produce dispersions, in which polymer clusters can be treated as separate chemical entities. Qualitative SAXS/SANS measurements indicate that in ~0.05–0.5% aqueous solutions PBS-PF2T polymer forms predominantly open two-dimensional aggregates with ribbon-like shape. The lateral dimension of aggregates is >30 nm and the thickness ~2.5 nm, which should be compared to the length of the polymer (~6 nm). The absorption and photophysical properties of PBS-PFT and PBS-PF2T are comparable to those of the corresponding nonionic alternating copolymers and, in particular, suggest that decreased fluorescence yields in these compared with PBS-PFP may result from the presence of the sulfur atom, which favors intersystem crossing. As was previously observed with PBS-PFP, these CPEs can be completely solubilized using nonionic surfactants. These two CPEs are currently being tested for applications in polymer–fullerene solar cells, in light-emitting electrochemical devices, and in fluorescence sensing. Results on these studies will be published shortly.

Acknowledgment. MAX-lab is acknowledged for the beamtime for the SAXS experiments. The SANS experiment was supported by EC (Contract RII3-CT-2003-505925). L.L.G.J. thanks the "Laboratório de Computação Avançada", of the Department of Physics of the University of Coimbra, for the computing facilities (Milipeia Cluster). We thank the FCT for the award of postdoctoral fellowships (to S.M.F. and L.L.G.J.). MEC and FEDER are thanked for financial support through Project MAT2004-03827 and POCI/FCT/FEDER through Project POCI/QUI/58291/2004. We are grateful for further funding for this collaboration through MEC/CRUP (Acções Integradas), GRICES, and DST (Acordo de Cooperação Científica e Tecnológica Portugal–India). Universidad de Burgos is also thanked for financial support of a short stay of M.J.T. at the University of Coimbra.

REFERENCES AND NOTES

(1) (a) Chen, L.; McBranch, D. W.; Wang, H.-L.; Helgenson, R.; Wudl, F.; Whitten, D. G. *Proc. Natl. Acad. Sci. U.S.A.* **1999**, *96*, 12287–12292. (b) Ambade, A. V.; Sandanaraj, B. S.; Klaikherd, A.; Thayumanavan, S. *Polym. Int.* **2007**, *56*, 474–481. (c) Bobacka, J. *Electroanalysis* **2006**, *1*, 7–18. (d) Liu, B.; Bazan, G. C. *J. Am. Chem. Soc.* **2006**, *128*, 1188–1196. (e) Liu, B.; Bazan, G. C. *Chem. Mater.* **2004**, *16*, 4467–4476. (f) Thomas, S. W.; Joly, G. D.; Swager, T. M. *Chem. Rev.* **2007**, *107*, 1339–1386.

(2) (a) Leclère, P.; Surin, M.; Brocorens, P.; Cavallini, M.; Biscarini, F.; Lazzaroni, R. *Mater. Sci. Eng., R* **2006**, *55*, 1–56. (b) Jaiswal, M.; Menon, R. *Polym. Int.* **2006**, *55*, 1371–1384. (c) Kulkarni, A. P.; Tonzola, C. J.; Babel, A.; Jenekhe, S. A. *Chem. Mater.* **2004**, *16*, 4556–4573. (d) Wohlgenannt, M.; Vardeny, Z. V. *J. Phys.: Condens. Matter* **2003**, *15*, R83−R107.

(3) (a) Coakley, K. M.; McGehee, M. D. *Chem. Mater.* **2004**, *16*, 4533–4542. (b) Van Hal, P. A.; Smits, E. C. P.; Geuns, T. C. T.; Akkerman, H. B.; De Brito, B. C.; Perissinotto, S.; Lanzani, G.; Kromemeijer, A. J.; Geskin, B.; Cornil, J.; Blom, P. W. M.; De Boer, B.; de Leeuw, D. *Nat. Nanotech.* **2008**, *3*, 749–752. (c) Zaumseil, J.; Sirringhaus, H. *Chem. Rev.* **2007**, *107*, 1296–1323. (d) Samuel, I. D. W.; Turnbull, G. A. *Chem. Rev.* **2007**, *107*, 1272–1295. (e) Günes, S.; Neugebauer, H.; Sariciftci, N. S. *Chem. Rev.* **2007**, *107*, 1324–1338.

(4) Burroughes, J. H.; Bradley, D. D. C.; Brown, A. R.; Marks, R. N.; Mackay, K.; Friend, R. H.; Burn, P. L.; Holmes, A. B. *Nature* **1990**, *347*, 539–541.

(5) Perepichka, I. F.; Perepichka, D. F.; Meng, H.; Wudl, F. *Adv. Mater.* **2005**, *17*, 2281–2305.

(6) (a) Najechalski, P.; Morel, Y.; Stéphan, O.; Baldeck, P. L. *Chem. Phys. Lett.* **2001**, *343*, 44–48. (b) Bliznyuk, V. N.; Carter, S. A.; Scott, J. C.; Klärner, G.; Miller, R. D.; Miller, D. C. *Macromolecules* **1999**, *32*, 361–369. (c) Bernius, M. T.; Inbasekaran, M.; O'Brien, J.; Wu, W. *Adv. Mater.* **2000**, *12*, 1737–1750. (d) Lieser, G.; Oda, M.; Miteva, T.; Meisel, A.; Nothofer, H.-G.; Scherf, U.; Neher, D. *Macromolecules* **2000**, *33*, 4490–4495. (e) Bernius, M. T.; Inbasekaran, M.; Woo, E.; Wu, W.; Wujkowski, L. *J. Mater. Sci.: Mater. Electron.* **2000**, *11*, 111–116. (f) Leclerc, M. *J. Polym. Sci., Part A: Polym. Chem.* **2001**, *39*, 2867–2873. (g) Scherf, U.; List, E. J. W. *Adv. Mater.* **2002**, *14*, 477–487. (h) Knaapila, M.; Winokur, M. J. *Adv. Polym. Sci.* **2008**, *212*, 227–272.

(7) Tirapattur, S.; Belletête, M.; Drolet, N.; Bouchard, J.; Ranger, M.; Leclerc, M.; Durocher, G. *J. Phys. Chem. B* **2002**, *106*, 8959–8966.

(8) (a) Andersson, M. R.; Berggren, M.; Inganäs, O.; Gustafsson, G.; Gustafsson-Carlberg, J. C.; Selse, D.; Hjertberg, T.; Wennerström, O. *Macromolecules* **1995**, *28*, 7525–7529. (b) Theander, M.; Inganäs, O.; Mammo, W.; Olinga, T.; Svensson, M.; Andersson, M. R. *J. Phys. Chem. B* **1999**, *103*, 7771–7780. (c) Monkman, A. P.; Burrows, H. D.; Hamblett, I.; Navaratnam, S.; Svensson, M.; Andersson, M. R. *J. Chem. Phys.* **2001**, *115*, 9046–9049. (d) Leclerc, M.; Fréchete, M.; Bergeron, J.-Y.; Ranger, M.; Lévesque, I.; Faid, K. *Macromol. Chem. Phys.* **1996**, *197*, 2077–2087.

(9) (a) Beljonne, D.; Shuai, Z.; Pourtois, G.; Brédas, J.-L. *J. Phys. Chem. A* **2001**, *105*, 3899–3907. (b) Burrows, H. D.; Seixas de Melo, J.; Serpa, C.; Arnaut, L. G.; Monkman, A. P.; Hamblett, I.; Navaratnam, S. *J. Chem. Phys.* **2001**, *115*, 9601–9606. (c) Seixas de Melo, J.; Burrows, H. D.; Svensson, M.; Andersson, M. R.; Monkman, A. P. *J. Chem. Phys.* **2003**, *118*, 1550–1556.

(10) Saadeh, H.; Goodson, T.; Yu, L. P. *Macromolecules* **1997**, *30*, 4608–4612.

(11) Kraabel, B.; Moses, D.; Heeger, A. J. *J. Chem. Phys.* **1995**, *103*, 5102–5108.

(12) Fonseca, S. M.; Pina, J.; Arnaut, L. G.; Seixas de Melo, J.; Burrows, H. D.; Chattopadhyay, N.; Alcácer, L.; Charas, A.; Morgado, J.; Monkman, A. P.; Asawapirom, U.; Scherf, U.; Edge, R.; Navaratnam, S. *J. Phys. Chem. B* **2006**, *110*, 8278–8283.

(13) (a) Baldo, M. A.; O'Brien, D. F.; You, Y.; Shoustikov, A.; Sibley, S.; Thompson, M. E.; Forrest, S. R. *Nature* **1998**, *395*, 151–154. (b) Cleave, V.; Yahioglu, G.; Le Barny, P.; Friend, R. H.; Tessler, N. *Adv. Mater.* **1999**, *11*, 285–288. (c) D'Andrade, B. *Nat. Photonics* **2006**, *1*, 33–34.

(14) (a) Bao, Z.; Dodabalapur, A.; Lovinger, A. J. *Appl. Phys. Lett.* **1996**, *69*, 4108–4110. (b) Sirringhaus, H.; Tessler, N.; Friend, R. H. *Science* **1998**, *280*, 1741–1744. (c) Medina, B. M.; Van Vooren, A.; Brocorens, P.; Gierschner, J.; Shkunov, M.; Heeney, M.; McCulloch, I.; Lazzaroni, R.; Cornil, J. *Chem. Mater.* **2007**, *19*, 4949–4956.

(15) Ma, W. L.; Yang, C. Y.; Gong, X.; Lee, K.; Heeger, A. J. *Adv. Funct. Mater.* **2005**, *15*, 1617–1622.

(16) Li, G.; Shrotria, V.; Huang, J.; Yao, Y.; Moriarty, T.; Emery, K.; Yang, Y. *Nat. Mater.* **2005**, *4*, 864–868.

(17) (a) Beaupré, S.; Leclerc, M. *Macromolecules* **2003**, *36*, 8986–8991. (b) Donat-Bouillud, A.; Lévesque, I.; Tao, Y.; D'Iorio, M.; Beaupré, S.; Blondin, P.; Ranger, M.; Bouchard, J.; Leclerc, M. *Chem. Mater.* **2000**, *12*, 1931–1936. (c) Lévesque, I.; Donat-Bouillud, A.; Tao, Y.; D'Iorio, M.; Beaupré, S.; Blondin, P.; Ranger, M.; Bouchard, J.; Leclerc, M. *Synth. Met.* **2001**, *122*, 79–81.

(18) (a) Charas, A.; Morgado, J.; Martinho, J. M. G.; Federov, A.; Alcácer, L.; Cacialli, F. *J. Mater. Chem.* **2002**, *12*, 3523–3527. (b) Charas, A.; Morgado, J.; Martinho, J. M. G.; Alcácer, L.; Lim, S. F.; Friend, R. H.; Cacialli, F. *Polymer* **2003**, *44*, 1843–1850. (c) Hou, Q.; Niu, H.; Huang, W. B.; Yang, W.; Yang, R. Q.; Yan, M.; Cao, Y. *Synth. Met.* **2003**, *135−136*, 185–186. (d) Vamvounis, G.; Schulz, G. L.; Holdcroft, S. *Macromolecules* **2004**, *37*, 8897–8902.

(19) (a) Pei, J.; Yu, W.-L.; Huang, W.; Heeger, A. J. *Chem. Commun.* **2000**, 1631–1632. (b) Pei, J.; Yu, W.-L.; Ni, J.; Lai, Y.-H.; Huang, W.; Heeger, A. J. *Macromolecules* **2001**, *34*, 7241–7248. (c) Liu, B.; Yu, W.-L.; Lai, Y.-H.; Huang, W. *Macromolecules* **2000**, *33*, 8945–8952.

(20) Ravirajan, P.; Haque, S. A.; Durrant, J. R.; Poplavskyy, D.; Bradley, D. D. C.; Nelson, J. *J. Appl. Phys.* **2004**, *95*, 1473–1480.

(21) Veres, J.; Ogirr, S.; Lloyd, G.; de Leeuw, D. *Chem. Mater.* **2004**, *16*, 4543–4555.

(22) (a) Kawase, T.; Shimoda, T.; Newsome, C.; Sirringhaus, H.; Friend, R. H. *Thin Solid Films* **2003**, *438/439*, 279–287. (b) Schubert, U. S. *Macromol. Rapid Commun.* **2005**, *26*, 237.

(23) (a) Ma, W.; Iyer, P. K.; Gong, X.; Liu, B.; Moses, D.; Bazan, G. C.; Heeger, A. J. *Adv. Mater.* **2005**, *17*, 274–277. (b) Huang, F.; Niu, Y.-H.; Zhang, Y.; Ka, J.-W.; Liu, M. S.; Jen, A. K.-Y. *Adv. Mater.* **2007**, *19*, 2010–2014.

(24) (a) Decher, G. *Science* **1997**, *277*, 1232–1237. (b) Baur, J. W.; Rubner, M. F.; Reynolds, J. R.; Kim, S. *Langmuir* **1999**, *15*, 6460–6469. (c) Kim, D. H.; Hernandez-Lopez, J. L.; Liu, G.; Mihov, G.; Zhi, L. J.; Bauer, R. E.; Grebel-Köhler, D.; Klapper, M.; Weil, T.; Müllen, K.; Mittler, S.; Knoll, W. *Macromol. Chem. Phys.* **2005**, *206*, 52–58.

(25) Burrows, H. D.; Fonseca, S. M.; Silva, C. L.; Pais, A. A. C. C.; Tapia, M. J.; Pradhan, S.; Scherf, U. *Phys. Chem. Chem. Phys.* **2008**, *10*, 4420–4428.

(26) (a) Burrows, H. D.; Lobo, V. M. M.; Pina, J.; Ramos, M. L.; Seixas de Melo, J.; Valente, A. J. M.; Tapia, M. J.; Pradhan, S.; Scherf, U. *Macromolecules* **2004**, *37*, 7425–7427. (b) Burrows, H. D.; Lobo, V. M. M.; Pina, J.; Ramos, M. L.; Seixas de Melo, J.; Valente, A. J. M.; Tapia, M. J.; Pradhan, S.; Scherf, U.; Hintschich, S. I.; Rothe, C.; Monkman, A. P. *Colloids Surf. A* **2005**, *270−271*, 61–66. (c) Tapia, M. J.; Burrows, H. D.; Knaapila, M.; Monkman, A. P.; Arroyo, A.; Pradhan, S.; Scherf, U.; Pinazo, A.; Pérez, L.; Morán, C. *Langmuir* **2006**, *22*, 10170–10174. (d) Burrows, H. D.; Tapia, M. J.; Silva, C. L.; Pais, A. A. C. C.; Fonseca, S. M.; Pina, J.; Seixas de Melo, J.; Wang, Y.; Marques, E. F.; Knaapila, M.; Monkman, A. P.; Garamus, V. M.; Pradhan, S.; Scherf, U. *J. Phys. Chem. B* **2007**, *111*, 4401–4410. (e) Burrows, H. D.; Tapia, M. J.; Fonseca, S. M.; Pradhan, S.; Scherf, U.; Silva, C. L.; Pais, A. A. C. C.; Valente, A. J. M.; Schillén, K.; Alfredsson, V.; Carnerup, A. M.; Tomsic, M.; Jamnik, A. *Langmuir* **2009**,submitted for publication.

(27) Knaapila, M.; Almásy, L.; Garamus, V. M.; Pearson, C.; Pradhan, S.; Petty, M. C.; Scherf, U.; Burrows, H. D.; Monkman, A. P. *J. Phys. Chem. B* **2006**, *110*, 10248–10257.

(28) Asawapirom, U.; Güntner, R.; Forster, M.; Farrell, T.; Scherf, U. *Synthesis* **2002**, *9*, 1136–1142.

(29) *Standards in Fluorescence Spectrometry*; Miller, J. N., Ed.; Chapman and Hall: London, 1981.

(30) Pina, J.; Burrows, H. D.; Becker, R. S.; Dias, F. B.; Maçanita, A. L.; Seixas de Melo, J. *J. Phys. Chem. B* **2006**, *110*, 6499–6505.

(31) Becker, R. S.; de Melo, J. S.; Maçanita, A. L.; Elisei, F. *J. Phys. Chem.* **1996**, *100*, 18683–18695.

(32) Seixas de Melo, J.; Fernandes, P. F. *J. Mol. Struct.* **2001**, *565*, 69–78.

(33) Striker, G.; Subramaniam, V.; Seidel, C. A. M.; Volkmer, A. *J. Phys. Chem. B* **1999**, *103*, 8612–8617.

(34) (a) Knaapila, M.; Svensson, C.; Barauskas, J.; Zackrisson, M.; Nielsen, S. S.; Toft, K. N.; Vestergaard, B.; Arleth, L.; Olsson, U.; Pedersen, J. S.; Cerenius, Y. submitted for publication. (b) Cerenius, Y.; Ståhl, K.; Svensson, L. A.; Ursby, T.; Oskarsson, Å.; Albertsson, J.; Liljas, A. *J. Synchrotron Radiat.* **2000**, *7*, 203–208.

(35) Stuhrmann, H. B.; Burkhardt, N.; Dietrich, G.; Junemann, R.; Meerwinck, W.; Schmitt, M.; Wadzack, J.; Willumeit, R.; Zhao, J.; Nierhaus, K. H. *Nucl. Instrum. Methods Phys. Res., Sect. A* **1995**, *A356*, 124–132.

(36) Glatter, O. *J. Appl. Crystallogr.* **1977**, *10*, 415–421.

(37) (a) Svergun, D. I. *J. Appl. Crystallogr.* **1992**, *25*, 495–503. (b) Svergun, D. I. *Biophys. J.* **1999**, *76*, 2879–2886.

(38) Robinson, R. A.; Stokes, R. H. *Electrolyte Solutions*, 2nd revised ed.; Dover Publications Inc.: New York, 2002.
(39) Barthel, J.; Feuerlein, F.; Neueder, R.; Wachter, R. *J. Solution Chem.* **1980**, *9*, 209–219.
(40) MOPAC2007, James J. P. Stewart, Stewart Computational Chemistry, version 8.087L; web HTTP://OpenMOPAC.net.
(41) Stewart, J. J. P. *J. Mol. Modeling* **2007**, *13*, 1173–1213.
(42) Pal, B.; Yen, W.-C.; Yang, J.-S.; Chao, C.-Y.; Hung, Y.-C.; Lin, S.-T.; Chuang, C.-H.; Chen, C.-W.; Su, W.-F. *Macromolecules* **2008**, *41*, 6664–6671.
(43) Belletête, M.; Beaupré, S.; Bouchard, J.; Blondin, P.; Leclerc, M.; Durocher, G. *J. Phys. Chem. B* **2000**, *104*, 9118–9125.
(44) (a) Fall, M.; Aaron, J.-J.; Dieng, M. M.; Párkányi, C. *Polymer* **2000**, *41*, 4047–4055. (b) Fonseca, S. M.; Eusébio, M. E.; Castro, R.; Burrows, H. D.; Tapia, M. J.; Olsson, U. *J. Colloid Interface Sci.* **2007**, *315*, 805–809.
(45) Poolmee, P.; Ehara, M.; Hannongbua, S.; Nakatsuji, H. *Polymer* **2005**, *46*, 6474–6481.
(46) (a) Tapia, M. J.; Burrows, H. D.; Valente, A. J. M.; Pradhan, S.; Scherf, U.; Lobo, V. M. M.; Pina, J.; Seixas de Melo, J. *J. Phys. Chem. B* **2005**, *109*, 19108–19115. (b) Monteserín, M.; Burrows, H. D.; Valente, A. J. M.; Lobo, V. M. M.; Mallavia, R.; Tapia, M. J.; García-Zubiri, I. X.; Di Paolo, R. E.; Maçanita, A. L. *J. Phys. Chem. B* **2007**, *111*, 13560–13569. (c) Monteserín, M.; Burrows, H. D.; Valente, A. J. M.; Mallavia, R.; Di Paolo, R. E.; Maçanita, A. L.; Tapia, M. J. *J. Phys. Chem. B* **2009**, *113*, 1294–1302.
(47) (a) Vink, H. *J. Chem. Soc., Faraday Trans. I* **1981**, *77*, 2439–2449. (b) Vink, H. *J. Chem. Soc., Faraday Trans. I* **1983**, *79*, 1403–1412. (c) Colby, R. H.; Boris, D. C.; Krause, W. E.; Tan, J. S. *J. Polym. Sci., Part B: Polym. Phys.* **1997**, *35*, 2951–2960.
(48) (a) Breiby, D. W.; Samuelsen, E. J.; Konovalov, O.; Struth, B. *Langmuir* **2004**, *20*, 4116–4123. (b) Knaapila, M.; Dias, F. B.; Garamus, V. M.; Almásy, L.; Torkkeli, M.; Leppänen, K.; Galbrecht, F.; Preis, E.; Burrows, H. D.; Scherf, U.; Monkman, A. P. *Macromolecules* **2007**, *40*, 9398–9405. (c) Ou-Yang, W.-C.; Chang, C.-S.; Chen, H.-L.; Tsao, C.-S.; Peng, K.-Y.; Chen, S.-A.; Han, C. C. *Phys. Rev. E* **2005**, *72*, 031802.
(49) Guilleaume, B.; Blaul, J.; Wittemann, M.; Rehahn, M.; Ballauff, M. *J. Phys.: Condens. Matter* **2000**, *12*, A245—A251.
(50) Rosen, M. J.; Cohen, A. W.; Dahanayake, M.; Hua, X.-Y. *J. Phys. Chem.* **1982**, *86*, 541–545.
(51) Dennier, G.; Scharber, M. C.; Brabec, C. J. *Adv. Mater.* **2009**, *21*, 1–16.
(52) (a) Gulgi, D. M.; Huie, R. E.; Neta, P.; Hungerbühler, H.; Asmus, K. D. *Chem. Phys. Lett.* **1994**, *223*, 511–516. (b) Eastoe, J.; Crooks, E. R.; Beeby, A.; Heenan, R. K. *Chem. Phys. Lett.* **1995**, *245*, 571–577.
(53) Crooks, E. R.; Eastoe, J.; Beeby, A. *J. Chem. Soc., Faraday Trans.* **1997**, *93*, 4131–4136.
(54) Mwaura, J. K.; Pinto, M. R.; Witker, D.; Ananthakrishnan, N.; Schanze, K. S.; Reynolds, J. R. *Langmuir* **2005**, *21*, 10119–10126.
(55) De la Maza, A.; Parra, J. L. *Biochem. J.* **1994**, *303*, 907–914.

AM800267N